Prediction of lifetime in perovskite thin films from early-time spatially resolved absolute-intensity photoluminescence images

Preetham Paul Sunkari
Hillhouse Group

CEI Graduate Fellow 2020-21 – Product of Lasting Value
& DIRECT Capstone Project

Introduction to perovskite solar cells:

In 2017, solar energy comprised 1.8% of the US electric supply with an installed capacity of 47 GW, which is a massive increase from 2011 when solar energy contributed less than 3 GW[2]. This surge in installations was a consequence of a plunge in the cost of solar energy from around ¢50/KWh to ¢16/KWh in those years. However, solar energy is still far from overtaking fossil fuels which generate electricity at just ¢6/KWh[2]. This urged the research community to develop cheaper and more efficient photovoltaic technologies, thus leading to the emergence of perovskite solar cells.

Mixed organic-inorganic halide perovskite solar cells, called perovskite solar cells (PSCs) in short, have shown a rapid increase in power conversion efficiencies from 14% to 25.2% in just seven years [5]. These materials have a common structure described with the formula ABX_3, where A is a monovalent organic or inorganic cation, B is a divalent inorganic cation with a smaller ionic size and X is a monovalent anion. The formula represents a large family of materials that can be made with different ions at A, B, and X sites in multiple compositions, thus offering great flexibility in tuning the electronic properties as needed. These promising materials demonstrate special optoelectronic properties – tunable direct bandgap for use in tandem solar cells, high absorption coefficient, and high defect tolerance – all of which helped them gather widespread attention in the recent years [4]. PSCs offer good efficiencies with low processing costs, making them ideal for cheap power generation. However, one major drawback that held them back is the use of toxic lead in these materials [4]. Moreover, poor stabilities of PSCs have been a major hindrance to their commercial deployment. Perovskite materials degrade rapidly within minutes when exposed to light in oxygen-rich and moist environments. So, researchers working with PSCs must conduct degradation experiments under a wide range of thermal, humidity, illumination, and oxygen stresses to understand the underlying degradation pathways and mitigate the stability issues

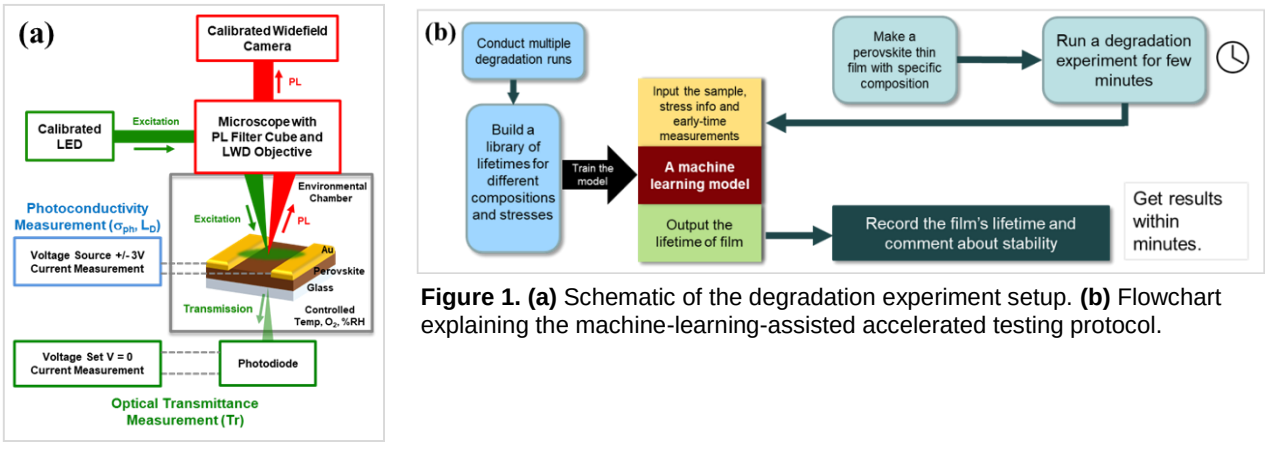

Figure 1. (a) Schematic of the degradation experiment setup. **(b)** Flowchart explaining the machine-learning-assisted accelerated testing protocol.

caused by them. Device failure studies, along with material-level analysis are fundamental for a comprehensive investigation of perovskite degradation.

In the Hillhouse group at the University of Washington, we examine the temporal decay of the material-level optoelectronic quality in perovskite thin films under different thermal, light, oxygen, and humidity stresses through in-situ photoluminescence (PL) and dark field (DF) microscopy, photoconductivity (PC), and film transmittance (Tr) measurements (Fig. 1a). Based on trends in this data, the possible dominating degrading factors and the lifetime of the film until failure can be obtained. Moreover, such a material-level characterization can be used for compositional screening of ions in the ABX_3 unit cell, to ultimately obtain the optimum material that would be stable and photo-efficient over a wide range of ambient conditions. But, some of these degradation experiments can go on for days, delaying the results. So, the overarching goal of these experiments is to develop an accelerated testing protocol using a machine learning model (Fig. 1b) that can predict the lifetime of a perovskite thin film, based on early time PC-PL-Tr measurements, sample properties like composition, grain size, etc, and the environmental stress factors like temperature, humidity, etc. This requires a vast and diverse dataset for training the model and identifying the dominant drivers of degradation. Once the model is trained on a rich dataset, it can be used to rapidly determine lifetimes of new perovskite materials over a wide range of environmental conditions using only short early-time measurements, instead of waiting long periods for the sample to degrade completely. This is important for commercial manufacturers to be able to predict the payback times for their perovskite modules using quick degradation tests, and hence such models play a crucial role in bringing these promising perovskite solar cells into the clean energy market.

Motivation:

Stoddard et. al. [1] (Fig. 2) from our group demonstrated a simple linear regression model trained on $MAPbI_3$ perovskite thin films, that can predict their lifetimes using early time diffusion length measurements, spatially-averaged pixel intensities of PL images and film transmittances. The article suggests the use of log (Ld85) which is the logarithm of the time it takes for the thin film's diffusion length to reach 85% of its initial value as a lifetime metric, which was surprisingly well-correlated with the aforementioned early-time features, despite a simple linear regression model had been used with a one-dimensional feature set. This indicates that more accurate and robust machine learning models can be built if more information can be leveraged from the PC-PL-Tr measurements. Especially, the early time PL images contain important spatial information which has been overlooked till now by these naïve linear regression models. For example, Fig 3 (a)-(d) shows two of many experiments in which although these two separate experiments were

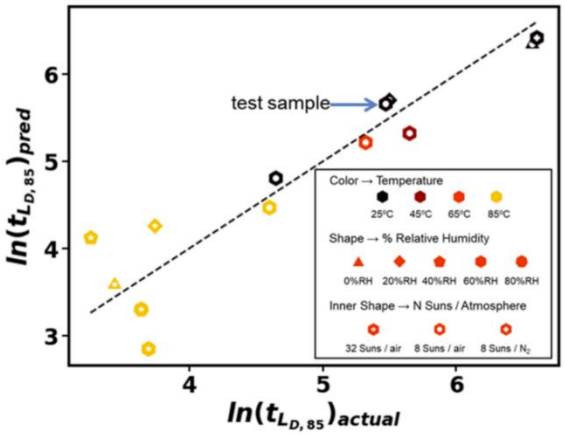

Figure 2. Linear Regression model used by Stoddard et. al. to predict $t_{Ld,85}$ [1]

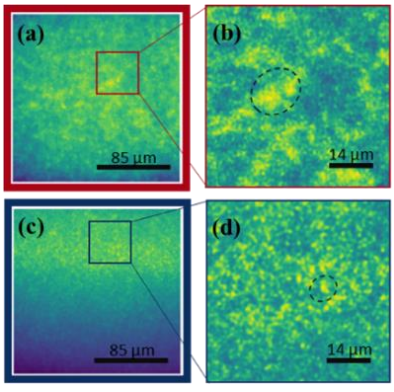

Figure 3. Photoluminescence (PL) images of MAPbI3 films taken under 25C, 60% RH, 8 Suns and air. **(a)** and **(b)** are replicates of MAPbI3 under same environ- mental stresses. **(b)** and **(d)** are enlarged versions of **(a)** and **(c)** respectively

conducted on the same material under the same environmental stresses, different sizes of bright PL clusters were observed at the beginning of the experiment. The two experiments in Fig 3 (a)-(d) were done on $MAPbI_3$ samples prepared at different times. This means the spatial heterogeneities in PL images could be encoding the differences in the film preparation conditions like the smoothness of substrates, the viscosity of inks used for spin coating, glovebox environment, etc. These heterogeneous features, which are much larger than the typical $MAPbI_3$ crystallite sizes (<0.1µm as obtained from XRD) and the grain sizes (<1µm as obtained from SEM), were termed 'super-grains'[3]. Such spatially and temporally resolved image data require special deep learning techniques to fully encode the spatial information into a one-dimensional feature array which we call the *"spatial PL feature array"* for subsequent use in a lifetime predictor.

Goal of the current project:

The current project aims to develop robust machine learning software tools that can encode the spatial-temporal heterogeneities usually observed in the early-time PL images of perovskite thin films during environmental degradation. Until now, only spatially-averaged PL image intensities have been used as features to predict log (Ld80) due to lack of relevant programming tools to encode the spatial information in these images. Hence, this project aims at using the PL images in their complete two-dimensional (2D) form as features, using convolutional neural networks, to avoid the loss of spatially resolved information.

Results and Discussion:

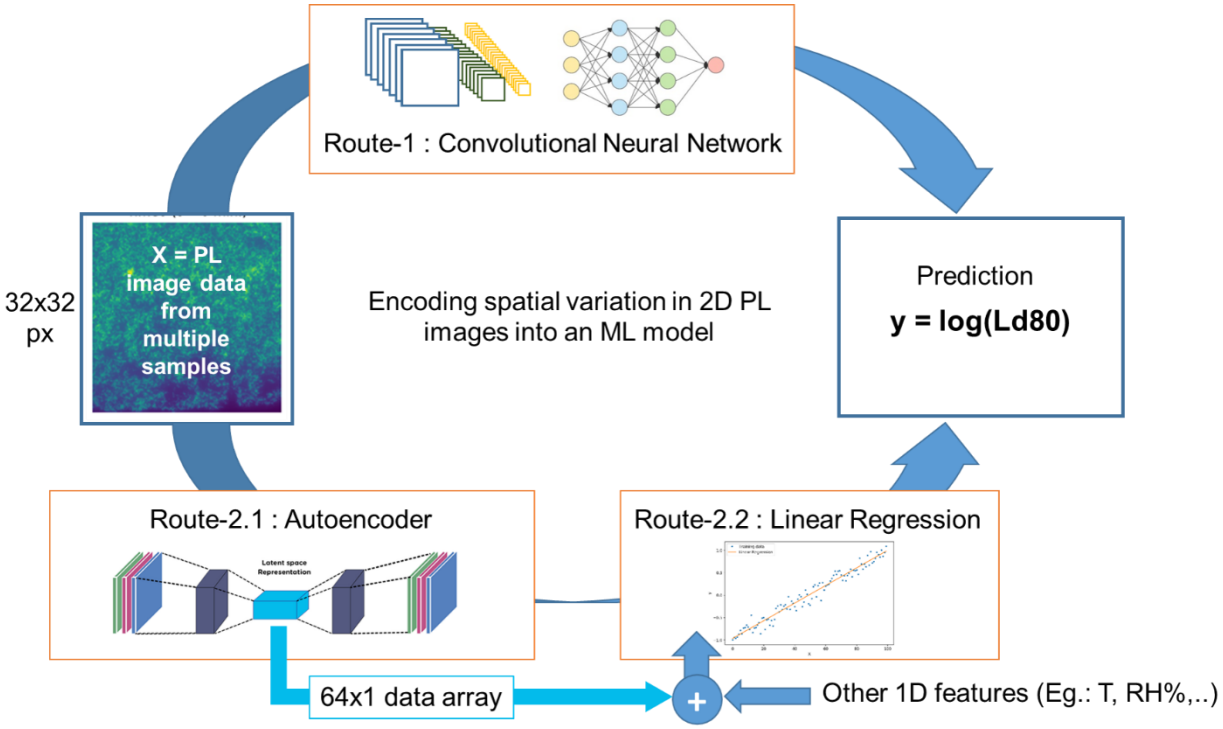

Figure 4. Two proposed routes to incorporate 2D PL images in a machine learning model to predict log (Ld80). Route-1 involves a traditional convolutional neural network (CNN) which outputs the log (Ld80) with the PL images as the feed input. Route-2 involves training an autoencoder (based on the CNN architecture) on the 2D PL image data to encode it into a 1D array, which can subsequently be fed into a linear regression model along with other scalar 1D features.

For this, our team, involved in the DIRECT capstone project, proposed two potential routes to incorporate the 2D PL features into a predictor machine learning model (Fig. 4). Route-1 uses a convolutional neural network (NN) that can receive the 2D PL image data as feed and predict a single scalar value of log (Ld80). Route-2 uses an autoencoder to encode the 2D PL image data into 1D spatial PL feature arrays, which can later be fed into a ridge linear regression model to predict the log (Ld80) value. For all models, the training and testing datasets consisted of a total N = 1245 number of degradation experiments, which were split randomly in 80:20 ratio to train and test the model respectively. Each experiment contains time series data of diffusion length (Ld) measurements, photoluminescence (PL) images and transmittance (Tr) measurements performed on $FA_yMA_xCs_{1-x-y}PbI_3$ samples under varying temperature (T), relative humidity (RH%), oxygen concentration (O2%), nitrogen concentration (N2%) and illumination intensity (Nsuns).

Use of spatial PL features in log (Ld80): Route-1 versus Route-2:

Each route has its own advantages and disadvantages depending on the size and the type of data. For our problem, route-2 has shown optimum results in terms of the test prediction error. Route-1 is apparently more vulnerable to overfitting compared to Route-2 and even the prediction parity plots (Fig. 5(a) and 5(c)) suggest the same. This is because Route-1 uses a single deep NN trained with 83,545 parameters or nodes spread across 9 hidden layers to predict log (Ld80), whereas Route-2 involves independent training of the autoencoder and the subsequent linear regression models. In the latter case, the autoencoder consists of 12,777 parameters of nodes spread across 15 hidden layers, takes in a downscaled feed image, encodes it into a 1D 64x1 array and attempts to reproduce the original image from it as output. Hence, the ground truths and the input data are identical for the autoencoder NNs. Later, the encoded 1D array obtained from the trained autoencoder is subsequently used in training the linear regression predictor. Thus, only 83 parameters corresponding to the input features fed into the linear regression are involved in the prediction of log (Ld80) in Route-2, making it less vulnerable to overfitting compared to Route-1. Figure 5(a)-(c) demonstrate how Route-2 performs significantly better than Route-1. The parity plots of predicted log (Ld80) versus observed log (Ld80) for Route-2 (Fig. 5(c)) show a better clustering of data-points along the x=y line compared to that in Route-1 (Fig. 5(a)). Moreover, the testing mean absolute error (MAE) in Route-2 has dropped to 25.74 % compared to 30.23 % in Route-1. With fewer parameters to train, Route-2 is faster to train than Route-1 and rapidly converges to low test MAEs even with large batch sizes and fewer iterations. A contrastingly low train MAE of 18.11% along with a decreased test MAE also suggest that the spatially resolved information on the PL image data is well captured by the Route-2's autoencoder augmented with a ridge regressor, compared to Route-1's sole deep CNN.

Validation of Route-2's feature set containing spatial PL features with one without spatial PL features using ridge linear regression

With Route-2 performing better than Route-1, it has become evident that low-bias modeling using linear regressors perform better by avoiding noise-fitting or over-fitting. To further establish Route-2 as the preferable method, we validated it using another ridge regression model, but without the PL spatial features. This is to verify how much improvement can be brought in the traditional linear regression models by incorporating spatial PL features obtained from the trained autoencoder. Table-1 below gives information about the features used for each linear regression model.

Table 1. Feature pool composition of the traditional ridge regression and Route-2 algorithms.

S. no.	Features	Number of features used	
		Traditional ridge regression (No spatial PL features)	**Route-2 Autoencoder + Ridge regression (including spatial PL features)**
1	A priori features (T, RH%, O2%, N2%, Nsuns, MA%, Cs%)	7	7
2	Early time measurements (Ld, PL and Tr measurements at t = 0, 5, 10 and 15 min.)	12	12
3	**Autoencoder features from time 0 PL images.**	**0**	**64**
	Total features	19	83

Fig 5(c) and Fig 5(d) show the log (Ld80) prediction parity plots for the Route-2 and the traditional case respectively. The model with the spatial PL features performed better with an improvement in the test MAE by 6.5%. Moreover, the datapoints align quite well along the x=y line in Fig. 5(c) compared to Fig. 5(d) indicating a better fit in the Route-2's model. Although the train MAE is contrastingly lower in the Route-2's model, the associated decrease in the test MAE assures that the addition of spatial PL features has not led to overfitting in the model. Fig. 5(e) and Fig 5(f) display the coefficient distribution of the top 8 and top 17 features selected by the ridge algorithm for the Route-2's and the traditional model's feature sets respectively. Fig. 5(e) shows that two spatial features obtained from the autoencoder – AE47 and AE63 replace the early time PL features seen in Fig. 5(f) as significant features indicating that the spatially resolved information in the early time PL images is highly correlated with log (Ld80).

Conclusion:

Our project results show that the spatial information in PL images of perovskite thin films can be effectively captured using autoencoders, and can be used to predict their lifetimes, the log (Ld80) values. This novel way of incorporating 2D PL images into predictor models using sequentially training disentangles the high-parametric convolutional methods essential for image-feature extraction, from the low-parametric linear predictor models, thus rendering an optimum combination of a synergistic low-bias and low-variation model. Although the Route-2's model already shows promising results, it can be further improved by tweaking the convolutional kernel parameters, activation function types and the hidden layer density of the CNN framework in the autoencoders to derive better performance. Moreover, employing ensemble methods like boosting and stacking can also result in improved accuracies.

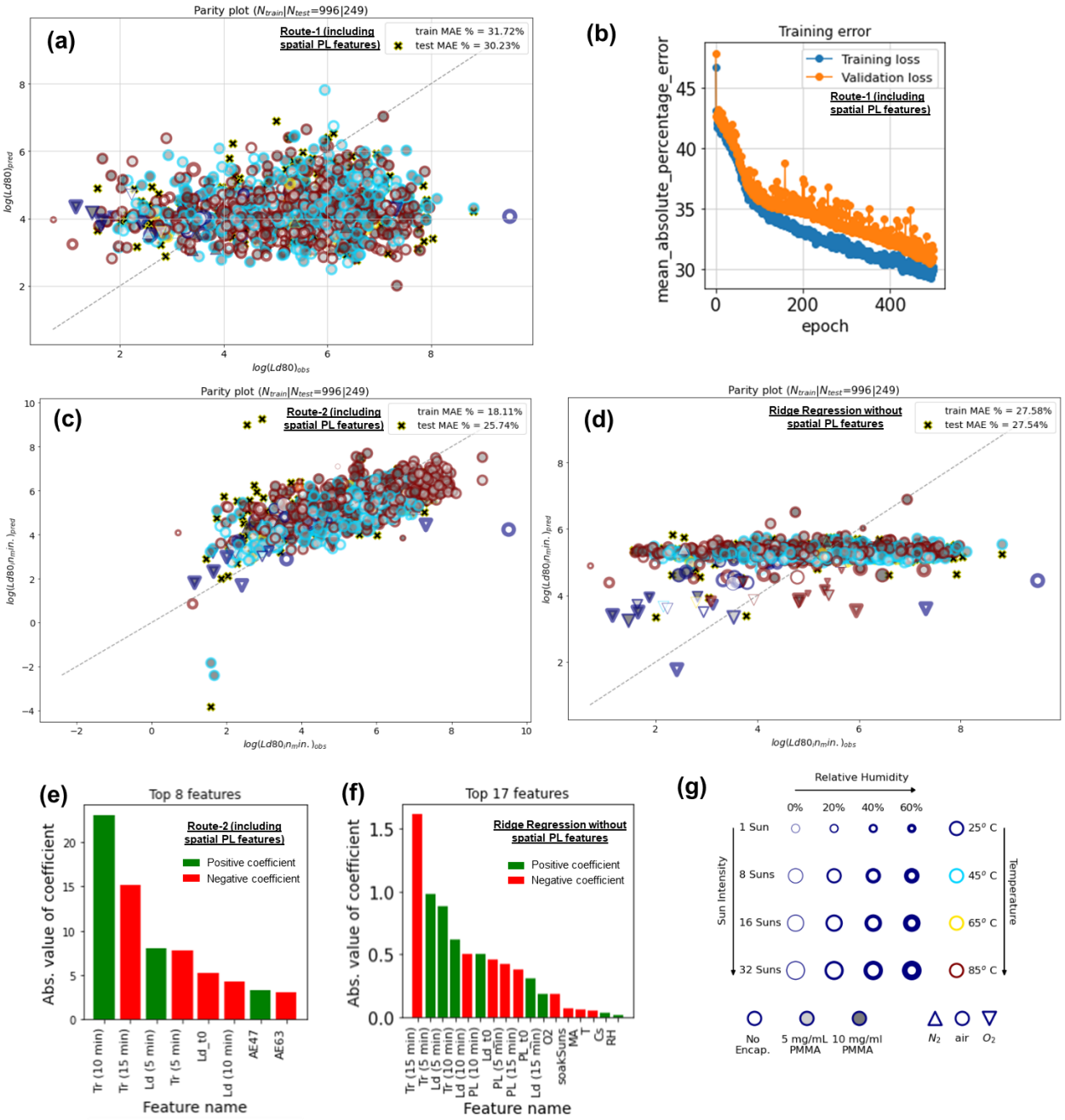

Figure 5. log (Ld80) prediction results for Route-1, Route-2 and validating traditional ridge regression without spatial PL features. **(a)** The log (Ld80) prediction parity plot for Route-1's algorithm (spatial PL features included). **(b)** Train and test MAE% evolution with training iteration count in Route-1 CNN's training. **(c)** The log (Ld80) prediction parity plot for Route-2's algorithm (spatial PL features included). **(d)** The log (Ld80) prediction parity plot for the traditional ridge linear regression algorithm (no spatial PL features included). **(e)** Coefficients of the top 8 features selected by the ridge regression algorithm in Route-2 corresponding to **(c)**. **(f)** Coefficients of the top 17 features selected by the ridge regression algorithm for the traditional dataset without spatial PL features, corresponding to **(d)**. **(g)** The legend for marker styling in the parity plot to describe the environmental conditions for each datapoint/degradation run.

Deliverables and intended audience:

This project is the first step in studying spatially resolved absolute intensity PL images to describe degradation in perovskite thin films. Currently, the perovskite research community lacks such software tools that can be used in accelerated testing protocols to study thin film degradation. So, the intended audience for the project deliverables would be researchers actively working in perovskite solar cells. However, the scope of the project can also be extended to other types of solar cells by training the models on new data, which we haven't checked yet. But, the framework proposed here to extract spatially resolved information from images can be implemented with any image data irrespective of the type of the material used. Thus, this project serves as an example to demonstrate how novel data science, image processing and programming tools can be used to facilitate traditional in-lab experiement-based research, in any field including clean energy.

The deliverables of the project are to be an open-source software package on Github that can perform the aforementioned analyses on image data provided by the user. Currently, since we are bound by a data disclosure agreement imposed by the Department of Energy who are the primary funders of the project, the full package will be published only after the end of the grant in December 2021. However, a truncated version of the software's results can be shared as the final CEI-PLV if confidentiality of it can be assured. As a part of the DIRECT capstone, this is also going to be presented in the eScience Institute Open-house Poster presentation on June 9th 2021. We are also planning to publish the results of this project in a relevant clean energy journal in neat future.

References:

1. Stoddard, Ryan. J. et al., 2020. Forecasting the Decay of Hybrid Perovskite Performance Using Optical Transmittance or Reflected Dark-Field Imaging. ACS energy letters, 5(3), pp.946–954.
2. U.S. Department of Energy, *SunShot 2030* program (https://www.energy.gov/eere/solar/sunshot-2030)
3. Jones, Timothy W et al., 2019. Lattice strain causes non-radiative losses in halide perovskites, Energy Environ. Sci., 2019,12, 596-606.
4. Ball, James M & Petrozza, Annamaria, 2016. Defects in perovskite-halides and their effects in solar cells. Nature Energy, 1(11), p.16149.
5. Best Research-Cell Efficiencies (National Renewable Energy Laboratory, 2020).